7164–7175 *Nucleic Acids Research, 2005, Vol. 33, No. 22*
doi:10.1093/nar/gki1013

Characterization of a catalytically efficient acidic RNA-cleaving deoxyribozyme

Srinivas A. Kandadai and Yingfu Li*

Department of Biochemistry and Biomedical Sciences and Department of Chemistry, McMaster University, 1200 Main Street West, Hamilton, Ontario, Canada L8N 3Z5

Received August 23, 2005; Revised November 11, 2005; Accepted November 25, 2005

ABSTRACT

We previously demonstrated—through the isolation of RNA-cleaving deoxyribozymes by *in vitro* selection that are catalytically active in highly acidic solutions—that DNA, despite its chemical simplicity, could perform catalysis under challenging chemical conditions [Liu,Z., Mei,S.H., Brennan,J.D. and Li,Y. (2003) *J. Am. Chem. Soc.* 125, 7539–7545]. One remarkable DNA molecule therefrom is pH4DZ1, a self-cleaving deoxyribozyme that exhibits a k_{obs} of $\sim$1 min^{-1} at pH 3.8. In this study, we carried out a series of experiments to examine the sequence and catalytic properties of this acidic deoxyribozyme. Extensive nucleotide truncation experiments indicated that pH4DZ1 was a considerably large deoxyribozyme, requiring $\sim$80 out of the original 123 nt for the optimal catalytic activity. A reselection experiment identified ten absolutely conserved nucleotides that are distributed in three catalytically crucial sequence elements. In addition, a *trans* deoxyribozyme was successfully designed. Comparison of the observed rate constant of pH4DZ1 with experimentally determined rate constant for the uncatalyzed reaction revealed that pH4DZ1 achieved a rate enhancement of $\sim$10^6-fold. This study provides valuable information about this low-pH-functional deoxyribozyme and paves way for further structural and mechanistic characterization of this unique catalytic DNA.

INTRODUCTION

Catalytic DNAs (also known as deoxyribozymes, DNAzymes or DNA enzymes) refer to single-stranded DNA molecules with a catalytic function (1–5). Through *in vitro* selection, a large number of deoxyribozymes have been isolated from random-sequence DNA libraries for catalyzing many chemical reactions that include cleavage and ligation of DNA or RNA strands (6–9), 5′-phosphorylation and 5′-adenylylation of DNA (10,11), porphyrin metallation (12) and thymine dimer repair (13). Deoxyribozymes are interesting molecules to study both for their relevance to inherent catalytic capabilities of nucleic acids and for their practical values. Indeed, a large number of deoxyribozymes are currently being studied as unique molecular tools for a variety of chemical and biological applications (2,3).

Despite very limited chemical functionalities, DNA is capable of executing efficient catalysis, reflected by the fact that many deoxyribozymes exhibit k_{cat} values at or above 1 min^{-1} (8,14–20). Most known deoxyribozymes are reported to function at or near physiological conditions. Encouraged by a study conducted by Jayasena and Gold in which self-cleaving ribozymes functional at low pH were isolated from a random-sequence RNA pool (21), we recently carried out an *in vitro* selection experiment to derive deoxyribozymes from a random-sequence DNA pool that could perform catalysis in a highly acidic solution (17). Several self-cleaving deoxyribozymes were indeed obtained for catalyzing RNA cleavage in highly acidic solutions. One of these deoxyribozymes, named pH4DZ1, is a highly effective catalyst, achieving a k_{obs} of $\sim$1 min^{-1} with a pH optimum of 3.8. DNA at this pH has considerably different properties due to the extensive protonation at the N1 atom of adenosine and the N3 atom of cytosine (1). Studying deoxyribozymes such as pH4DZ1 that have unusual catalytic capability is expected not only to expand our general understanding of catalysis by both natural and artificial polymers, but also to recover useful information that could facilitate the development of deoxyribozymes for applications under unusual chemical conditions.

Here we report on a comprehensive characterization of the catalytic and sequence properties of pH4DZ1. We conducted a series of experiments designed to achieve the following four specific goals: (i) minimizing the size of pH4DZ1, (ii) identifying the functionally essential nucleotides within its sequence, (iii) designing a *trans*-acting deoxyribozyme system and (iv) assessing the rate enhancement achieved by pH4DZ1. The results from these experiments are described below.

*To whom correspondence should be addressed. Tel: +1 905 525 9140; Fax: +1 905 522 9033; Email: liying@mcmaster.ca

MATERIALS AND METHODS

Oligonucleotides and chemical reagents

Standard and modified DNA oligonucleotides were prepared by automated chemical synthesis (HHMI-Keck Biotechnology Resource Laboratory, Yale University; Central Facility, McMaster University) using general phosphoramidite chemistry. The partially randomized libraries used for reselection were synthesized using the following mixture of the four standard phosphoramidites (produced by manual mixing): 76% of the wild-type nucleotide, 8% of each of the remaining 3 nt using protocol described previously (10). DNA oligonucleotides were purified by 10% denaturing (8 M urea) PAGE. The triisopropylsilyloxymethyl (TOM) group of the RNA linkage was removed using the previously reported method (18). Nucleoside 5′-triphosphates, [γ-^{32}P]ATP and [α-^{32}P]dGTP were purchased from Amersham Pharmacia. T4 DNA ligase, T4 polynucleotide kinase (PNK) and *Taq* DNA polymerase were purchased from MBI Fermentas. All other chemical reagents were purchased from Sigma and used without further purification. Water used throughout the study was deionized.

All catalytic assays and the reselection experiment were carried out in the selection/assay buffer that contained a final concentration of 50 mM citric acid (pH 3.8, 25°C), 400 mM NaCl and 10 mM $CdCl_2$ (2× stock solution was used). The stop solution contains 40 mM EDTA (pH 8.0, 25°C), 8 M urea, 90 mM Tris, 90 mM boric acid, 10% sucrose (w/v), 0.025% xylene cyanol and 0.025% bromophenol blue (stored as 2× stock solution). The DNA phosphorylation reaction was performed in 50 mM Tris–HCl (pH 7.6, 25°C), 10 mM $MgCl_2$, 5 mM DTT, 0.1 mM spermidine and 0.1 mM EDTA (pH 8.0, 25°C) (supplied by the manufacturer as 10× stock solution). The DNA ligation reaction was carried out in 40 mM Tris–HCl (pH 7.8, 25°C), 0.5 mM ATP, 10 mM $MgCl_2$ and 10 mM DTT (also supplied by the manufacturer as 10× stock solution).

Assessing the activity of *cis* deoxyribozymes

All the *cis* pH4DZ1 variants (the substrate was covalently attached to each deoxyribozyme) required for the sequence truncation and mutation studies in discussed in the Results section were constructed in the following way. A synthetic oligonucleotide as the donor DNA (at final concentration of 4 μM) was labeled at the 5′ end with 10 μCi of [γ-^{32}P]ATP and PNK (0.1 U/μl, final concentration; total reaction volume is 50 μl). Thus phosphorylated DNA was ligated with a required substrate in the presence of appropriate DNA template (acceptor:donor:template = 1:1:1) and T4 DNA ligase at room temperature for 1 h. The ligated deoxyribozyme construct was purified by 10% denaturing PAGE. The deoxyribozyme (1 pmol) in water was heated at 90°C for 30 s and then cooled to room temperature for 5 min. The RNA cleavage reaction was initiated by the addition of the 2× selection/assay buffer. The final DNA concentration was set at ~0.1 μM. At 0.1, 1, 10, 100 and 1000 min, an aliquot of the reaction mixture was withdrawn and quenched with the 2× stop solution, followed by freezing at −20°C. Cleavage products were separated by 10% denaturing PAGE and product yields were determined by quantitating product bands using a PhosphoImager and ImageQuant software (Molcular Dynamics). The catalytic ability of each deoxyribozyme was scored using the following scheme. Any deoxyribozyme construct exhibiting a k_{obs} of 0.1 min^{-1} (10% cleavage in 1 min) or above was given the highest score at '+++++'; mutant deoxyribozymes with a k_{obs} at or above 0.01 (≥10% cleavage in 10 min), 0.001 (≥10% cleavage in 100 min), 0.0001 min^{-1} (≥10% cleavage in 1000 min) but below the threshold k_{obs} value set for the next upper level were scored '++++', '+++' and '++', respectively; those with a k_{obs} below 0.0001 min^{-1} (<10% cleavage in 1000 min) were given a '+'; molecules that produced no cleavage bands after incubation for 1000 min were denoted by a '−'. At least two independent assays were conducted for each deoxyribozyme construct to ensure that each scoring was accurate.

Selective deoxyribozymes were chosen for determination of accurate initial rate constants. Each deoxyribozyme was allowed to cleave in the selection/assay buffer. The reaction was stopped at some time intervals chosen to obtain data points that were under 20% completion of the reaction. The rate constants (k_{obs}) were then calculated by plotting the natural logarithm of the fraction of DNA that remained uncleaved versus the reaction time. The negative slope of the line produced by a least-squares fit to the data was taken as the rate constant.

Reselection protocol

Reselection of mutant deoxyribozymes from a partially randomized, pH4DZ1-based library was carried out largely according to the previously reported selection protocol (17) with some variations. Briefly, for the first round of selection, 500 pmol of gel-purified library was phosphorylated at the 5′ end with 20 μCi of [γ-^{32}P]ATP and PNK at 37°C for 30 min. Non-radioactive ATP was then added into the solution (to a final concentration of 1 mM) and the mixture was further incubated for 20 min at 37°C. The phosphorylated DNA library was ligated to a substrate named S3 (see the Results section) using T4 DNA ligase. The ligated DNA was purified by denaturing 10% PAGE and was resuspended in 100 μl of water. Two parallel selections were conducted, one with 1 min incubation time and the other with 5 h incubation time. In each selection, 100 pmol of ligated DNA in 40 μl was heated at 90°C for 30 s and cooled to room temperature for 5 min. After the addition of 40 μl of 2× selection/assay buffer and incubation for either 1 min or 5 h at room temperature, the reaction was quenched by the addition of the 2× stop solution. The 3′ cleavage fragment was isolated by 10% denaturing PAGE, amplified by PCR and then made into single-stranded DNA, all according to the previous protocol (17).

For the subsequent rounds, the cleavage reaction was performed as described above. The DNA populations from both 1 min and 5 h selections after the 4th round were amplified by PCR and cloned into the plasmid pUC57 using the T/A cloning method. Plasmids containing individual catalysts were isolated using the 96-well PerfectPrep kit (Eppendorf). Deoxyribozyme inserts were sequenced on a CEQ 2000XL DNA sequencer (Beckman-Coulter) using the CEQ Quick Start Kit (Beckman-Coulter) according to the protocol provided by the manufacturer.

DMS methylation interference assay

The method to be described below was adapted from a previously published protocol (22,23). A truncated pH4DZ1, named EC2 (see the Results section for its sequence), was used for this experiment. The *cis* deoxyribozyme was constructed by ligating a DNA oligonucleotide denoted donor EC2 (its sequence is 5′-GGGGA GAAAC ATCTT TGCGG GATAA GGCCG CCGAT AGAGC GGAAG CGACT TGGTT GTAGC TGAT-3′) with the substrate S1. The ligation reaction was performed as follows. Donor EC2 (500 pmol) was first phosphorylated with a trace amount of [γ-^{32}P]ATP and PNK (0.1 U/μl, final concentration; total reaction volume is 50 μl) for 20 min at 37°C, followed by the addition of non-radioactive ATP to a final concentration of 1 mM. The mixture was further incubated for 20 min to ensure complete phosphorylation. PNK was then inactivated by heating the reaction mixture at 90°C for 5 min. This mixture was directly added to a 200 μl ligation solution containing 600 pmol of the DNA template T2 (5′-GTTTC TCCCC TCGAA CCATA) and 550 pmol of S1 (see the Results section for its sequence). The ligation was initiated by the addition of T4 DNA ligase (0.2 U/μl, final concentration) and continued at room temperature for 5 h. The ligated DNA was subsequently purified by denaturing 10% PAGE.

The above ligated EC2 (100 pmol) in water was heated at 90°C for 30 s and cooled to room temperature for 5 min. The cleavage reaction was initiated by the addition of the reaction buffer, followed by incubation at room temperature for 5 min. The reaction was then quenched by EDTA (30 mM, final concentration). The DNA in the solution was recovered by ethanol precipitation, resuspended in water (500 μl), heated at 90°C for 1 min and cooled to room temperature quickly. An equal volume of 0.4% (v/v) DMS (freshly made) was added and the resultant mixture was incubated at room temperature for 40 min. Thus treated DNA was recovered by ethanol precipitation. This DNA sample was labeled as the 'control'.

Another 100 pmol of uncleaved EC2 was methylated with DMS in the same fashion. After the recovery by ethanol precipitation, the methylated DNA was then allowed to cleave for 5 min with the addition of the 2× reaction/assay buffer. After quenching with EDTA (30 mM, final concentration), the DNA was recovered by ethanol precipitation. This DNA sample was labeled as the 'test'. Both the control and test DNA samples were phosphorylated with 20 μCi of [γ-^{32}P]ATP and PNK at 37°C for 20 min. After purification by 10% denaturing PAGE, both the control DNA and the test DNA were dissolved in 10% (v/v) piperidine (100 μl, freshly made) and heated at 90°C for 30 min. The resultant cleavage products were dried under vacuum. The dried pellet was resuspended in 25 μl of H_2O and evaporated to dryness under vacuum. This step was repeated one more time. Both the control and test samples were then subjected to denaturing 10% PAGE analysis to reveal piperidine-mediated cleavage fragments.

The k_{obs} value of the *trans* deoxyribozyme under a single-turnover condition

5′-^{32}P-phosphorylated S2 (0.5 μM, 35 nt) and ET1 (25 μM; for the sequences of S2 and ET1, see the Results section) in H_2O were heated at 90°C for 30 s, cooled to room temperature, followed by the addition of the 2× selection/assay buffer. After pre-determined time intervals, a fraction of the reaction solution was taken, quenched with the stop solution and stored at −20°C. These mixtures were finally analyzed by 10% denaturing PAGE. The rate constant (k_{obs}) was determined by plotting the natural logarithm of the fraction of S2 that remained uncleaved versus the reaction time (the negative slope of the least-squares fit was taken as the initial rate constant).

Assessing the multiple-turnover capability of the trans deoxyribozyme

The chimeric DNA/RNA substrate S2 used for the multiple-turnover experiment was double purified by PAGE. After gel elution and ethanol precipitation steps, the potential contaminants (such as salts and EDTA) were removed from the substrate by centrifugation using a spin column (Nanosep 3K Omega, Pall Corp., Ann Arbor, Michigan). The final concentration of the substrate S2 was varied from 500, 1000, 5000 and 10 000 nM (plus trace amount of 5′-^{32}P-labeled S2) at fixed ET1 (*trans*-acting deoxyribozyme) concentration (100 nM). In a typical reaction, S2 and ET1 in H_2O were heated at 90°C for 30 s, cooled to room temperature before the addition of the 2× reaction/assay buffer. After incubation at room temperature for 0, 0.5, 1, 2, 4 and 8 h, the reaction was quenched with the 2× stop solution and stored at −20°C. The reaction mixtures were finally analyzed by 10% denaturing PAGE.

RESULTS

Scoring catalytic activity of mutant deoxyribozyme constructs

We purposely divide the sequence of pH4DZ1 into two domains labeled in Figure 1A as 'substrate' (italicized letters) and 'catalyst' (normal letters), to simply reflect the fact that this catalytic DNA was originally derived using a library of 100 nt single-stranded DNA molecules covalently joined to the 23 nt substrate (denoted S1). The two sequence stretches shown in lower-case letters were used as the primer-binding sites for the PCR during the original *in vitro* selection. For convenience, we have marked the nucleotides in the substrate domain from −1 to −23 in the 3′-to-5′ direction and the ones in the catalyst domain from 1 to 100 in the 5′-to-3′ direction. The specific number assigned to each nucleotide remains unchanged throughout this report, even though many mutant deoxyribozyme constructs contained one or more truncated nucleotides. It should be noted that the substrate domain contains three special nucleotides: the DABCYL-containing deoxyribothymidine (**Q**; DABCYL: 4-(4-dimethylaminophenylazo)benzoic acid), adenine ribonucleotide (**A**) and the fluorescein-containing deoxyribothymidine (**F**) at the −8th, −9th and −10th positions, respectively. The ribonucleotide is the cleavage site while **F** and **Q** provide a setting for fluorescence signaling upon catalysis for future biosensing applications.

The activity of all mutant deoxyribozymes, analyzed using synthetic DNA oligonucleotides containing an internal ^{32}P-labeled phosphodiester, was scored as described in 'Materials and Methods' (see the insert in Figure 1B). Generally speaking, a mutant deoxyribozyme with a score of +++++ or ++++ is

Figure 1. The nucleotide sequence of pH4DZ1 and the activity of various truncated deoxyribozymes. (**A**) The primary sequence of pH4DZ1. The self-cleaving deoxyribozyme is divided into the 'substrate' domain, S1 (italicized letters; numbered −1 to −23 in the 3′–5′ direction), and the 'catalyst' domain (normal letters only; numbered 1 to 100 in the 5′–3′ direction). The lower-case letters are the primer-binding sequences for the original *in vitro* selection experiment. (**B**) Truncating nucleotides from the 5′ end of the catalyst domain. (**C**) Removing nucleotides from the 3′ end of the catalyst domain. The reference sequence is pH4DZ1. Underlined nucleotides are the sequence region under investigation, with the vertical arrow pointing to the mutated sequences. The identities of the nucleotides represented by black bars are omitted for clarity. The name of each mutant deoxyribozyme is listed next to its altered sequence. The activity of each construct in this figure (as well as in all remaining figures) is scored using the activity map shown as the insert in (B). All individual deoxyribozymes were constructed by ligating substrate S1 with a relevant 5′-^{32}P-labeled synthetic oligonucleotide. F = Fluorescein-dT, Q = DABCYL-dT and A = Adenine ribonucleotide

regarded as an efficient catalyst ($k_{obs} \geqslant 0.01$ min^{-1}) while a sequence scored +++ or lower is treated as a poor catalyst. It should be noted that the activity-scoring scheme is adopted to simplify the task of comparing relative activities of all deoxyribozyme mutants tested in this report. More precise catalytic rate constants of selective mutant deoxyribozymes were determined and will be discussed later.

Truncating nucleotides in the catalyst domain

In the original *in vitro* selection experiment, we utilized a library of 123 nt single-stranded DNA molecules. The use of a relatively long DNA sequence to construct the DNA library was based on the assumption that a large DNA sequence may result in a better catalyst. Since all known RNA-cleaving deoxyribozymes isolated under neutral pH conditions (such as 8–17 and 10–23) are fairly small in size, we wondered whether the low-pH-functional pH4DZ1 also used relatively limited nucleotides to construct its catalytic core. We therefore carried out comprehensive sequence truncation experiments (including systematically removing terminal or internal nucleotides from the catalyst domain) and the results are shown in Figures 1 and 2.

The effects of deleting nucleotides from the 5′ end of the catalyst domain were assessed first and the data are presented in Figure 1B. The original primer-binding sequence was completely dispensable (EC1, +++++; E: enzyme; C: *cis*-acting). In fact, deleting the next 16 nt also produced no significant effect because EC2 (28 nt deletion, +++++) and EC3 (31 nt deletion, also +++++) exhibited the activity that was similar to pH4DZ1. Removing the next 3 nt (EC4, +++) resulted in a deoxyribozyme that suffered ∼100-fold activity reduction. These results indicate that the 31 nt from G_1 to G_{31} have little relevance to the active structure and catalysis of pH4DZ1 while G_{32}, A_{33}, G_{34}, though not catalytically essential, make important contributions to the full activity of the deoxyribozyme.

Progressive removal of nucleotides from the 3′ end of the catalyst domain was carried out next and the data are presented

Figure 2. Activity of deoxyribozyme mutants with sequential internal nucleotide truncation. EC6 was used as the reference deoxyribozyme. Each short dash represents a deleted nucleotide in comparison to the sequence of EC6. Each mutant deoxyribozyme contained continuous 6 nt deletion. The name of each mutant deoxyribozyme is listed next to its sequence. The activity of each mutant deoxyribozyme is scored using the activity map given in Figure 1B. All individual deoxyribozymes were constructed by ligating substrate S1 with a relevant 5′-^{32}P-labeled synthetic oligonucleotide. The three regions shaded in grey are identified as the sequence elements that contain functionally most crucial nucleotides based on the observation that each 6 nt removal resulted in either complete loss of activity (−) or near-complete loss of activity (10^4 activity reduction, i.e. from +++++ to +).

in Figure 1C. Truncating as many as 10 nt from the 3′ terminus had no apparent effect on the catalytic activity as the mutant deoxyribozymes EC5-7 (having 5, 8 and 10 nucleotides deleted from the 3′ end of the deoxyribozyme) all retained full activity. Removing five additional nucleotides from the same end reduced the catalytic activity by ~100-fold (EC8, +++) while truncating five more nucleotides nearly abolished the RNA-cleaving activity (EC9, +). These results indicate even some of the nucleotides located within the 3′-primer-binding site are required for the full catalytic activity of the deoxyribozyme.

Deletion of internal nucleotides

The terminal nucleotide truncation experiments demonstrated that all functionally important nucleotides (required to support full catalytic activity of pH4DZ1) within the catalyst domain are located between G_{31} and G_{90}. To determine whether some of the internal nucleotides could also be removed, we carried out a 'deletion walking' experiment and the data are shown in Figure 2. More specifically, we conducted a series of sequential, 6 nt deletions, starting from G_{16} and ending at A_{91}. Each new deletion had a 3 nt overlap with the previous deletion. EC6 was used as the reference deoxyribozyme for this experiment.

Surprisingly, the deletion walking experiment clearly indicated that pH4DZ1 could not tolerate well a continuous 6 nt deletion anywhere between G_{31} and A_{91}. Most of the 6 nt deletion mutants caused at least 1000-fold activity reduction (++ or lower), and only EC21 (++++), EC29 (+++) and EC33 (+++) had the activity above ++. These results suggest that a large number of nucleotides in this region participate in interactions critical to the folding and/or catalysis of the deoxyribozyme. More importantly, the deletion walking experiment has identified three separate sequence elements (shaded in grey in Figure 2) containing the nucleotides that appeared to be most crucial to the function of the deoxyribozyme as each 6 nt deletion within these elements caused either complete loss of activity (−) or near-complete loss of activity (+).

Identification of functionally essential nucleotides by *in vitro* selection

We turned our attention next to the identification of individual nucleotides within the three crucial sequence elements highlighted in grey in Figure 2. Since there are a total of 30 nt in these regions, it would be extremely time-consuming to assess the functionality of individual nucleotides using single-nucleotide mutation strategy. For this consideration, we chose to conduct an *in vitro* selection experiment. A chemically synthesized, partially mutagenized pH4DZ1 DNA library was constructed in which (i) the nonessential nucleotides between 1 and 25 were removed and (ii) every position in G_{32}–T_{43}, C_{56}–G_{67} and G_{80}–T_{86} (upper-case letters in large font, Figure 3B) was mutagenized at a mutation rate of 24% (76% of the wild-type nucleotide and 8% each of the other 3 nt) following a previous protocol (10).

The *in vitro* selection scheme was similar to that used for the isolation of pH4DZ1 (17) (re-shown in Figure 3A) except for the use of different DNA molecules. Briefly, the DNA library L1 was ligated to substrate S3, in the presence of the template T1 and T4 DNA ligase, to yield 105 nt S3-L1 constructs

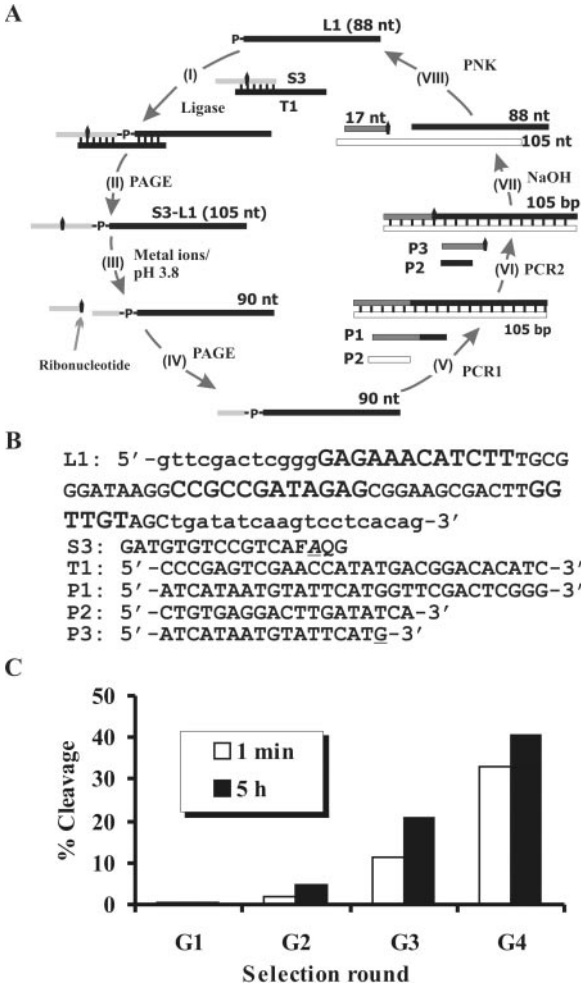

Figure 3. *In vitro* selection of functional pH4DZ1 mutants. (**A**) Selection scheme. Each selection cycle consists of steps I–VIII. (I) 88 nt DNA L1 is ligated to 17 nt substrate S3. (II) Ligated 105 nt DNA is isolated by PAGE. (III) Purified 105 nt DNA is incubated with divalent metal ions for RNA cleavage. (IV) The 90 nt 3′-cleavage fragment is isolated by PAGE. (V) The recovered 90 nt DNA is amplified by PCR using primers P1 and P2. (VI) 105 bp PCR product in (V) is further amplified by PCR using primers P2 and P3 to introduce a ribonucleotide linkage embedded in front of the L1 sequence. (VII) The resulting double-stranded DNAs are treated with NaOH to cleave the ribonucleotide linkage. (VIII) The cleavage fragments are phosphorylated at 5′ end, and used to initiate the next round. (**B**) All the DNA sequences used for *in vitro* selection. The lower-case letters in L1 are primer-binding sites; the letters in larger fonts in L1 are partially randomized nucleotides. Other nucleotides in L1 are not randomized. The underlined letters are ribonucleotides. (**C**) Selection progress. The white bars are the selection with a 1 min RNA cleavage time while the black bars are for 5 h selection. The *x*-axis represents the selection round; the *y*-axis plots the percentage of detected RNA cleavage in each selection round.

(step I). After purification by 10% denaturing PAGE (step II), the S3-L1 chimeras were allowed to cleave in the selection buffer (step III). The 3′ cleavage fragment (90 nt) was first purified by 10% denaturing PAGE (step IV) and then amplified by two successive rounds of PCR (steps V and VI). The purpose of the second PCR was to introduce a ribonucleotide right before the start of L1 sequence so that single-stranded L1 could be regenerated by alkaline digestion (VII). After 5′-phosphorylation by PNK, the single-stranded L1 molecules were used to initiate a new round of selective amplification. The sequences of all the DNA molecules used for the *in vitro*

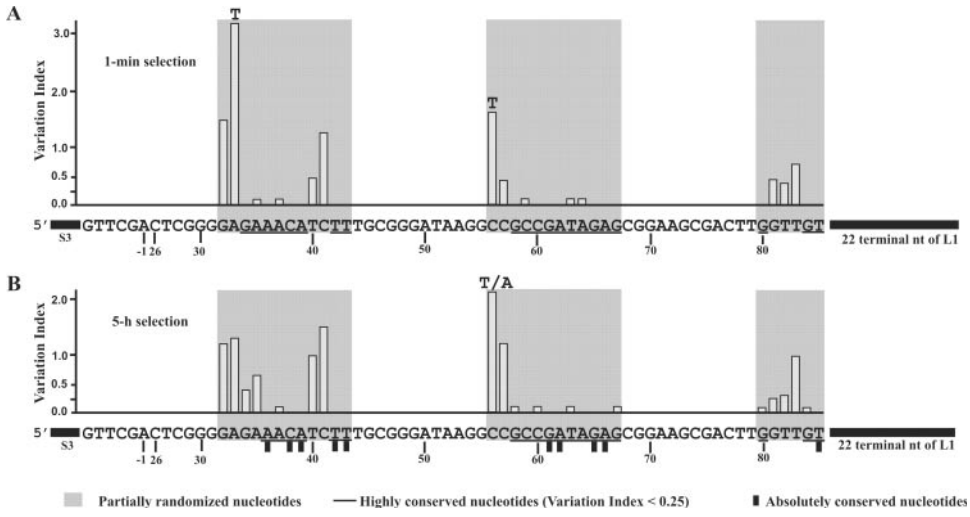

Figure 4. Sequence analysis of terminal pools from both 1 min and 5 h selection. The variation index (VI) complied for 1 min selection (**A**) and 5 h selection (**B**) upon sequencing ~40 clones from each G4 population. The variation index was calculated by dividing the observed mutation rate at each position by 24% (the mutation rate of the starting library). The wild-type sequence is shown at the bottom of each chart (the last 22 nt at the 3′ constant region is omitted for clarity). Only nucleotides shaded in the grey zones are partially mutagenized. The underlined nucleotides are the nucleotides either absolutely conserved (VI = 0) or highly conserved (VI $\leqslant$ 0.25). The letter or letters placed at the top of the VI bars that are significantly larger than 1 (meaning these nucleotides were hyper-mutagenized) indicated the dominant nucleotides in the selected deoxyribozyme clones at the given positions. The short black bars beneath certain nucleotides in (B) denote the nucleotides that are absolutely conserved in both selections.

selection are given in Figure 3B. It is important to note that new primer-binding sequences were used in the reselection to avoid cross-contamination by the wild-type pH4DZ1 that exists in our lab as the possible contaminant. In particular, the last 19 nt of L1 sequence have never been used for any pH4DZ1 mutant construct, and this will certainly eliminate any chance for cross-contamination by any deoxyribozyme studied before the *in vitro* selection experiment.

Two separate *in vitro* selection experiments were conducted under identical settings except that the permissive reaction times were different. In the first selection, the reaction time for RNA cleavage was set at 1 min (denoted 1 min selection); in the second selection, a 5 h reaction time was used (denoted 5 h selection). Since 5 h selection is much less stringent than 1 min selection, we expected that the former should allow more base mutations than the later, which should help identify the nucleotides that are very crucial to the function of the deoxyribozyme. In contrast, 1 min selection should identify the nucleotides that are important to the optimal activity of the deoxyribozyme. Progress of each selection is shown in Figure 3C. After four rounds of selective amplification, both populations reached ~35% reaction completion.

Approximately 40 clones were sequenced from both the cloned 1 min and 5 h pools. On average, each sequence acquired approximately five mutations as compared to the original sequence while only one sequence in each population contained all wild-type nucleotides (data not shown). A statistical analysis of the sequences of all isolated clones are given in Figure 4 where the original sequence of the shortened pH4DZ1 is shown with the variation index (V.I., a measure of variability) plotted for each base position (22). The variation index was calculated by dividing the observed mutation rate (in percentage) at each position by 24%, which is the mutation rate of the starting library. A variation index of 0 indicates that the base is absolutely conserved in all the sequenced clones. In theory, if there are no constrictions on a base position, the variability observed within the sequenced population should be equivalent to the mutation rate (i.e. 24%); in such cases the variation index would be 1. Values greater than 1 could indicate that mutations confer a selective advantage over the original base. By far the majority of positions from both reselections have variation indices between 0 and 1. We arbitrarily chose values of below 0.25 to indicate high-level conservation (underlined nucleotides in Figure 4).

Three points are worth commenting. First, the overall variation index pattern for both 1 min and 5 h populations is very similar. As expected, more mutations occurred in 1 min clones as compared to 5 h clones; however, 5 h selection only produced mutations at four more nucleotide positions (mutations were observed in 18 positions in 5 h clones versus 14 in 1 min clones). The major difference between the two variation index plots is that 5 h clones had two more major mutation sites in G_{34} and A_{35}. Interestingly, the variation index at A_{33} in the 1 min selection was very high (3.2) as compared to 5 h selection (1.4). Furthermore, A_{33} was almost exclusively mutated to T in 1 min clones while the mutation at A_{33} in 5 h clones was variable. This suggests that A33T mutation conveys selective advantage for optimal catalytic function. Similarly, C_{56} was mainly mutated to T in 1 min clones whereas C_{56} was mutated either to A or T in 5 h clones. Second, this low-pH-functional deoxyribozyme could not tolerate a large number of base mutations in the three sequence elements. Twenty-one of the 30 nt exhibited a V.I. of 0.25 or lower in 1 min clones. The number of extremely conserved nucleotides only experienced a subtle drop to 19 nt in 5 h clones. Third, there are 10 nt that were absolutely conserved across all 1 min and 5 h clones (labeled with a black bar beneath each concerned nucleotide in Figure 4). Undoubtedly, these nucleotides are the residues that are most crucial to the structure and/or function of pH4DZ1.

Chemical probing using dimethyl sulfate

As discussed above, the deletion walking and reselection experiments identified many highly conserved nucleotides that must be important to the structure and function of pH4DZ1. Noticeably, many of these nucleobases are guanines. Therefore, it is certain that some of these guanine residues are critically involved in the structural folding and catalytic function of this deoxyribozyme.

We sought to use the methylation interference approach to obtain additional evidence that can further implicate the functional roles of the crucial guanine residues in pH4DZ1. More specifically, we wanted to assess the level of tolerance by a fully functional deoxyribozyme construct EC2 (+++++) towards the methylation of the N7 atom of each of its component guanine residues. Hypothetically, the methyltion of N7 of a guanine residue is prohibited if any one of the following three scenarios applies. First, the N7 atom is directly involved in a tertiary interaction that is essential for structure folding or catalytic function. Second, the N7 atom is located in a defined structural arrangement that cannot tolerate the bulky methyl group. Third, the positive charge introduced by the methylation disrupts the vital electronic landscape where the guanine residue is located. In contrast, the guanine residues located in functionally insignificant sequence motifs should not produce significant methylation interference effect.

For each methylation interference experiment, we used a set of two DNA samples, which are denoted 'control' and 'test' (22,23). The control sample was subjected to a procedure illustrated in Figure 5A. For illustration purpose, only two identical deoxyribozyme molecules, EC2A and EC2B each containing two hypothetical guanine residues shown as 'g' and 'G', were drawn. When these two molecules were allowed to cleave under permissive reaction conditions (step 1), the 3′ cleavage product (P2A and P2B from EC2A and EC2B, respectively) and 5′-cleavage fragment (P1) of the *cis* deoxyribozyme would be produced. The resulted DNA fragments were then subjected to treatment with DMS in water (step 2). Under this condition single-stranded DNA should exist in unfolded random-coil state and the 'g' and 'G' residues should be methylated with approximately equal probability. The methylation was purposely carried out at a DMS concentration that should only allow the methylation of one guanine per DNA molecule. P2A and P2B, isolated from the reaction mixture by denaturing PAGE following the phosphorylation with [γ-^{32}P]ATP/PNK (step 3), were then allowed to cleave in the presence of piperidine (step 4, which cleaves the DNA strand at all methylated guanines). Thus generated DNA fragments were finally analyzed by denaturing PAGE. Because methylation was performed after the catalysis step, radioactive DNA fragment P2A1 and P2B1 (corresponding to the respective cleavage product at the 'g' and 'G' residues) should be observed at relatively equal intensity.

The test sample was treated according to the scheme shown in Figure 5B. The procedural difference for the two samples was the order of the first two steps: methylation with DMS was carried out with the deoxyribozyme construct before the self-cleavage reaction for the test sample (while for the control sample, the self-cleavage reaction was conducted first). If the methylation at a particular guanine residue (represented herein by the 'g' residue) hindered the self-cleaving activity of the deoxyribozyme, no RNA cleavage or significantly reduced RNA cleavage would occur. As a result, no cleaved product from the 'g' location would be obtained. This would eventually lead to a missing DNA band or a band with significantly reduced intensity on denaturing PAGE. Similarly, methylated guanines that enhanced the activity of the deoxyribozyme would be identified by their increased band visibility.

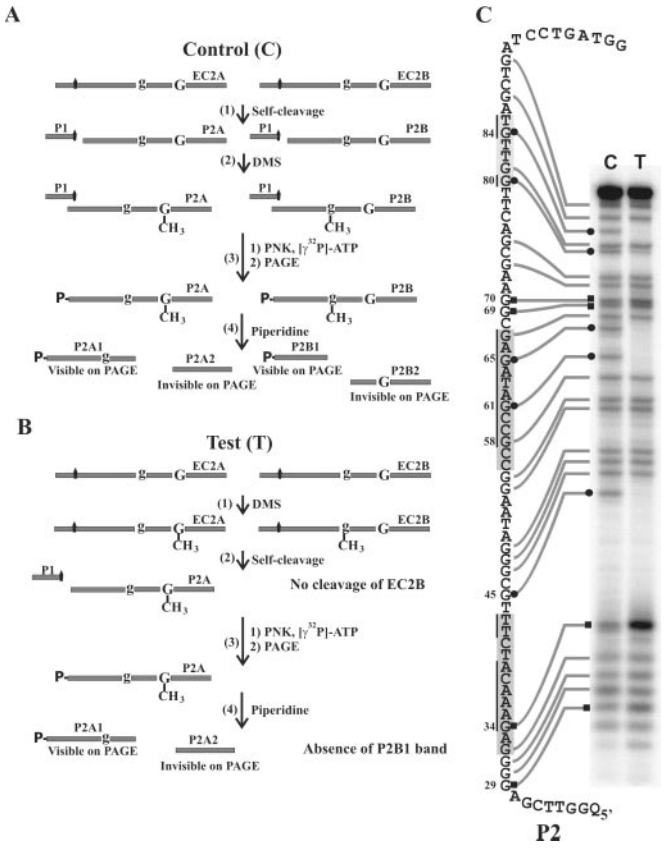

Figure 5. Methylation interference. (**A**) and (**B**) outline the experimental scheme for obtaining DNA ladders to be analyzed as 'Lane C' and 'Lane T' in (**C**). Briefly, the 3′-cleavage fragment obtained from EC2 treated with DMS before (Test-T) or after (Control-C) the cleavage reaction was performed and labeled at the 5′ end with ^{32}P. Under our reaction condition, DMS only methylated the N7 atom of one guanine per deoxyribozyme molecule on average. Methylated guanines were cleaved by piperidine at 90°C and cleaved fragments were resolved by 10% denaturing PAGE. Methylated guanines that disrupt deoxyribozyme activity appear missing or lighter in lane T than lane C. Filled black circles at the left side of the gel (and next to a concerned nucleotide) indicate the DNA bands with significantly reduced intensity in T lanes while the black square labels the DNA band that had a significantly enhanced intensity in the T lane. EC2 was used for this experiment. The sequence of the cleavage fragment P2 in (C) was drawn using the same labeling scheme given in Figure 4.

The PAGE analysis result of methylation interference experiment is given in Figure 5C. Nucleotides with noticeably reduced band intensity were labeled with a filled circle; those with enhanced intensity were labeled with a filled square. No cleavage band was observed in T lane for the following four guanine residues: G_{45}, G_{61}, G_{65} and G_{84}. This finding indicates that pH4DZ1 cannot tolerate the methylation of the N7 atom of these guanines. The intensity of the DNA band corresponding to G_{80} was visible but significantly reduced, suggesting that the methylation of this guanine residue considerably reduced

the activity of the deoxyribozyme. Interestingly, there are four cleaved DNA bands in T lane that showed a noticeable enhancement in intensity over the same band in C lane and they corresponded to G_{29}, G_{34}, G_{69} and G_{70}. G_{34} in particular had the most drastic intensity enhancement. As a control experiment, we also treated the cleavage fragment directly with piperidine without a DMS methylation step and found no breakage at any of these guanosine residues (data not shown). This analysis indicates that each of these residues was not selectively depurinated at pH 3.8. Since methylation of N7 atom of a guanine residue introduces both a positive charge and a relatively bulky methyl group on the guanine, the intensity enhancement may have two possible reasons. One is that the introduction of the methyl group brings in a better spatial arrangement of the guanine in the folded deoxyribozyme structure, and the other is that the positive charge introduced strengthens an interaction that is important to the structure and function of the deoxyribozyme. We favor the second option based on the following three considerations. First, there are a total of four guanines with intensity enhancement. It is hard to believe that pH4DZ1, by chance, explores the better spatial arrangement introduced by the methyl group at four different locations. Second, the same hyper-methylation has not been observed for the two self-phosphorylating deoxyribozymes recently characterized by our lab (22), suggesting that this phenomenon may be an exclusive property of this low-pH-functional deoxyribozyme. Third, at pH 3.8, the extensive protonations at adenines and cytosines may make the catalytic core of the deoxyribozyme highly positively charged and the methylation at a relevant guanine could significantly strengthen this property. However, the precise reason for the enhancement could not be pinpointed at this moment and will be investigated in greater detail in our future research efforts.

Not surprisingly, most of methylation-interfering guanines reside in the three crucial sequence elements identified by the deletion walking experiment. The only exception was G_{45} which is located 1 nt away from the first such sequence element. Taken together, the methylation interference experiment provided strong evidence that further implicated the functional involvement of many important guanine residues identified by mutational analysis and reselection.

Sequence truncation and nucleotide permutation of the substrate domain

We also examined functional relevance of nucleotides in the substrate region and the data are shown in Figure 6. This region contains two specially modified deoxyribonucleotides Q_{-8} (DABCYL-dT) and F_{-10} (fluorescein-dT) as well as the lone ribonucleotide $\underline{A}_{-9}$ (ribo-A). Deoxyribozyme constructs in which either fluorescein (EC34) or dabcyl (EC35) or both (data not shown) were removed exhibited no self-cleaving activity. These results indicate that both the fluorescein and DABCYL labels are crucial to the deoxyribozyme function. Similarly, we found that $\underline{A}_{-9}$ is also a nucleotide specifically required for the deoxyribozyme function, reflected by the inability to self-cleave seen with the three constructs in which the cleavage site was changed to cytidine ribonucleotide (EC36), guanosine ribonucleotide (EC37) and uridine ribonucleotide (EC38). These findings imply that the adenine attached to ribose is involved in highly specific interactions that are part of the active deoxyribozyme structure.

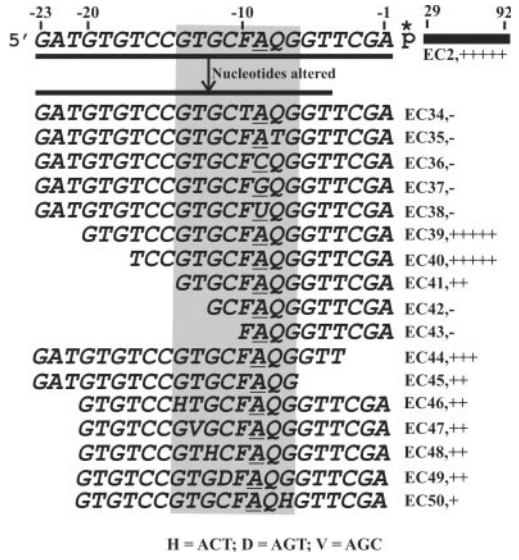

Figure 6. Nucleotide alteration within the substrate domain. Different nucleotides from both the 5′ and 3′ ends of the substrate were altered (deletion or mutation) to identify the catalytically important nucleotides. H = equimolar mixture of A, C and T; D = equimolar mixture of A, G and T; and V = equimolar mixture of A, G and C. $\underline{A}$ = Adenine ribonucleotide, $\underline{G}$ = Guanine ribonucleotide, $\underline{C}$ = Cytosine ribonucleotide and $\underline{U}$ = Uracil ribonucleotide. Nucleotides shaded in grey are catalytically important.

Several deoxyribozyme constructs with sequential nucleotide truncations from either 5′ or 3′ end of the substrate domain were next examined. Removing the first 6 nt from the 5′ end 3 nt each time (EC39 and EC40, both +++++) produced no effect on the catalytic activity. The construct with three more nucleotides deleted from the same end (EC41, ++) exhibited an activity reduction by ~1000-fold. Further truncations of the remaining nucleotides two at each time completely deactivated the deoxyribozyme (EC42 and EC43, both).

Interestingly, all nucleotides downstream of the cleavage site in the substrate domain were required for the optimal function of the deoxyribozyme, as the deletion of even 2 nt from the 3′ end of the substrate domain (EC44, +++) lowered the catalytic activity by ~100-fold. Removal of three more nucleotides from the same end (EC45, ++) led to a new construct whose activity was weakened by ~1000-fold.

Finally, we examined the functional roles of the five standard nucleotides in the region shaded in grey, G_{-7}, C_{-11}, G_{-12}, T_{-13} and G_{-14}, by nucleotide permutations. All these nucleotides appear to play important roles in the catalytic function of the deoxyribozyme, because mutating any of these nucleotides to the mixture of the three remaining residues (G_{-7} to H_{-7}, EC50, +; C_{-11} to D_{-11}, EC49, ++; G_{-12} to H_{-12}, EC48, ++; T_{-13} to V_{-13}, EC47, ++; G_{-14} to H_{-14}, EC48, ++; H = ACT, D = AGT) weakened the RNA-cleaving activity by at least 1000-fold. Together, these results indicate that a majority of nucleotides in the substrate domain are required for the optimal function of the deoxyribozyme. It is possible that these nucleotides are engaged in extensive tertiary interactions responsible for substrate–catalyst recognition.

Engineering of a *trans*-acting deoxyribozyme

Almost all the *cis*-acting RNA-cleaving DNA enzymes that operate under neutral pH conditions can be re-engineered into *trans*-acting deoxyribozymes with multiple-turnover capability (8,24–28). We therefore sought to design a *trans* system for pH4DZ1. From sequence truncation data presented in Figure 1B, it is apparent that nucleotides from G_1 to G_{32} are completely dispensable. Based on this observation, we first designed a *trans* substrate S2 by moving the first 12 nt of the catalyst domain to the end of the S1 sequence. The newly designed 35 nt substrate S2 was used for all the *trans* experiments.

Since all known *trans* deoxyribozymes interact with their RNA substrates through the formation of two Watson–Crick helices (one upstream and downstream of the cleavage site), we wondered whether we could design a *trans* deoxyribozyme that can engage S2 by forming a stable Watson–Crick duplex. For this consideration, ET1 (E: enzyme; T: *trans*-acting) was made that was able to form 17 bp duplex as shown in Figure 7A. Gel-shifting experiment confirmed the binding of S2 and ET1 at neutral pH (data not shown). Under the single-turnover setting of ET1:S2 = 50:1 ([ET1] = 25 μM; [S2] = 0.5 μM), ET1 exhibited a k_{obs} of 0.40 min^{-1} (initial rate, see Figure 7B), which is almost identical to the catalytic rate constant displayed by the *cis* pH4DZ1 (a k_{obs} of ~1 min^{-1}) (17). This finding indicates that the nucleotides added to the 5′ end of the ET1 did not significantly affect the folding and the catalytic function of the deoxyribozyme.

We then sought to assess the dispensability of the artificially imposed duplex that engaged the deoxyribozyme to the substrate by assaying the relative activity of several deoxyribozyme constructs in which the nucleotides at the 5′ end were progressively truncated (ET2–ET6). Removing up to 12 nt did not significantly affect the deoxyribozyme activity in *trans* as ET2–ET4 exhibited an activity that was identical to ET1. Deletion of one more nucleotide (ET5) resulted in about 3-fold activity reduction. Further nucleotide truncation (ET6) essentially rendered the *trans* deoxyribozyme inactive. These results demonstrated that the formation of artificially engineering Watson–Crick duplex is not necessary to the function of the *trans* deoxyribozyme. Consistently, ET1 and ET4 were fully functional when S1 was used instead of S2 (S1 does not contain the last 12 nucleotides of S2).

Experiment shown in Figure 7C was then conducted to examine whether ET1 had multiple-turnover capability. When 100 nM of ET1 was incubated with 10 000 nM of S2 for 0.5, 1, 2, 4 and 8 h, 272, 535, 1157, 2067 and 3504 nM of the cleavage product P1 were produced (Figure 7C). Similar experiments were also conducted using other substrate concentrations (500, 1000 and 5000 nM) and the calculated turnover data are summarized in Supplementary Table 1. Overall, our results indicated that ET1 indeed had multiple-turnover capability. For instance, the deoxyribozyme produced 35 turnovers in 8 h at the substrate concentration of 10 000 nM (100% cleavage under this setting can result in a total of 100 turnovers). We noted that the rate of turnover appeared to be smaller than the observed rate constant for single-turnover rate. For example, 2.7 turnovers in 30 min at [S2] = 10 000 nM (representing an excessive substrate concentration; [ET1] = 100 nM) correspond to a rate of turnover of

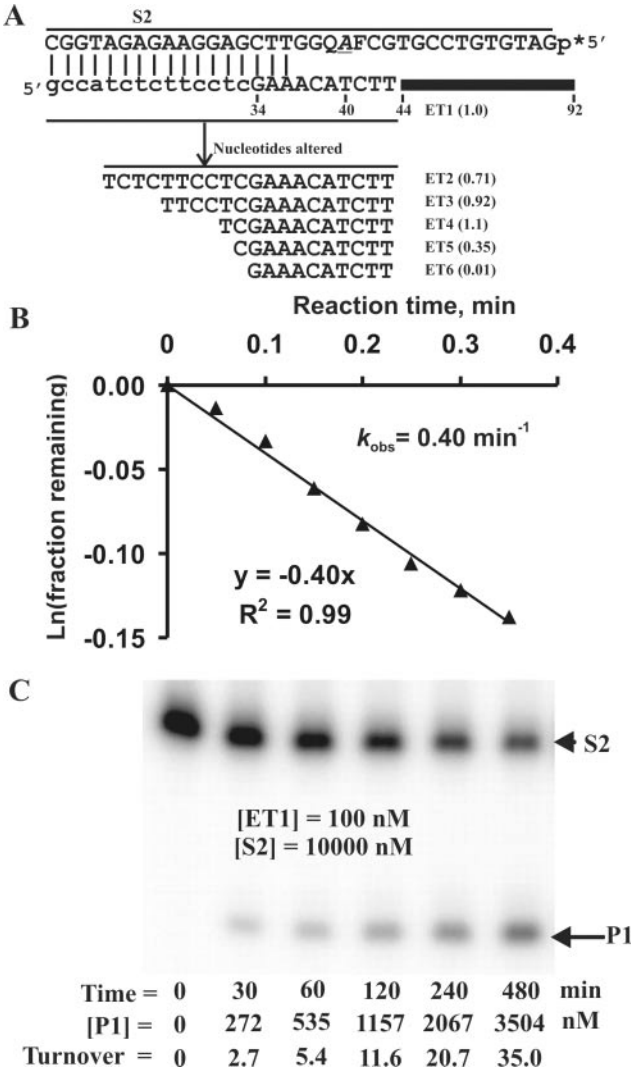

Figure 7. A *trans*-acting catalytic system. (**A**) Designing a *trans*-acting pH4DZ1 system. A 35 nt substrate S2 was designed that contained the sequence of S1 and the first 12 nt from the catalyst domain in the original pH4DZ1. The 72 nt *trans*-acting deoxyribozyme ET1 was constructed that contained the nucleotides from 34–92 of the original pH4DZ1 as well as 14 additional nucleotides (lower-case letters) introduced at the 5′ end of the deoxyribozyme. The first 17 nucleotides were designed to form Watson–Crick base pairs with the last 17 nt of S2. Various ET1 mutants with nucleotides truncated from the 5′ end were tested under single-turnover condition (S2 and each deoxyribozyme were set to be 0.5 and 25 μM, respectively). The activity of all deoxyribozymes was normalized to that of ET1. (**B**) Plot for deriving single-turnover k_{obs} of S2/ET1. Substrate S2 (0.5 μM) was incubated with ET1 (25 μM) in the selection/assay buffer [50 mM Citric acid (pH 3.8), at 25°C, 400 mM NaCl and 10 mM $CdCl_2$]. At indicated time points, an aliquot of the reaction was withdrawn, quenched and stored at −20°C. After collecting samples, the reaction mixture was analyzed by 10% denaturing PAGE. The formation of the cleavage product P1 (which is radioactive) was quantitated using ImageQuant Software. The *x*-axis represents reaction time in min and *y*-axis plots natural logarithm of the fraction of S1 that remained uncleaved at the various reaction times. Each data point represents the average value of two independent experiments. The negative slope of the least-squares fit is taken as the first-order initial rate constant, which was found to be 0.40 min^{-1}. (**C**) PAGE analysis of the multiple-turnover capability of S2/ET1 system. S2 (10 000 nM) (in the presence of trace amount of 5′-^{32}P-labeled S2) were incubated with 100 nM ET1 in the selection/assay buffer for 0, 30, 60, 120, 240 and 480 min and the reaction mixture was analyzed by 10% denaturing PAGE. The concentration of P1 was calculated using ImageQuant Software. The number of turnovers by ET2 was then computed as [P1]/[ET2].

0.09 min^{-1}, which is about 23% of the single-turnover rate of 0.4 min^{-1} (Figure 7B).

We also assessed the pH dependence and metal specificity of ET1/S2 under single-turnover condition and found that the *trans*-acting system exhibited essentially identical properties described previously for pH4DZ1 (data not shown) (17). This result shows that truncation of nonessential nucleotides did not alter these two key properties of the deoxyribozyme.

Initial rate constant and rate enhancement of representative deoxyribozymes

Up to this point, the activities of all mutant deoxyribozymes were compared using the semi-quantitative scoring scheme given in Figure 1B. To assess the accuracy of the method, we sought to determine the first-order initial rate constant for the 13 representative deoxyribozymes listed in Table 1. The chosen deoxyribozymes cover all activity classes: six from '+++++' class (pH4DZ1, EC1, EC2, EC6, EC12 and EC39), one each from '++++' and '+++' classes (EC21 and EC29, respectively), two from '++' class (EC46 and EC48) and two from '+' class (EC9 and EC14). The plot for deriving k_{obs} of EC6 (the most efficient mutant pH4DZ1) is shown as Figure 8A. All the catalytic rate constants, in duplicate (shown as the second and third columns in Table 1, with the fourth column being the average value), were derived in the same fashion. The data given in Table 1 are consistent with the activities of the concerned deoxyribozymes assigned by the qualitative scoring method, with no exception. For example, the deoxyribozyme variants scored with a '+++++' activity indeed exhibit a catalytic rate constant of 0.1 min^{-1} or above, with EC6 and EC12 at the opposite ends with a k_{obs} of 1.2 min^{-1} and 0.12 min^{-1}, respectively.

Table 1. Initial rate constants for various mutants of pH4DZ1

DNAzyme name	k_{obs}, min^{-1} repeat 1	k_{obs}, min^{-1}, repeat 2	k_{obs}, min^{-1}, average	Rate enhancement
pH4DZ1	1.1	0.95	1.0	1.7×10^6
EC1	0.16	0.15	0.16	2.6×10^5
EC2	0.96	0.90	0.93	1.6×10^6
EC6	1.1	1.2	1.2	1.9×10^6
EC9	0.000031	0.000028	0.000030	4.9×10
EC12	0.10	0.14	0.12	2.0×10^5
EC14	0.000030	0.000017	0.000024	3.9×10
EC21	0.020	0.016	0.018	3.0×10^4
EC29	0.0026	0.0027	0.0027	4.4×10^3
EC39	0.84	0.77	0.81	1.3×10^6
EC46	0.00086	0.00088	0.00087	1.5×10^3
EC48	0.00046	0.00048	0.00047	7.8×10^2
ET1/S2	0.40	0.41	0.40	6.8×10^5
S1 only	0.00000048	0.00000071	0.00000060	

Each deoxyribozyme was allowed to cleave in the selection/assay buffer. The reaction was stopped at certain time intervals to obtain data points under 20% reaction completion. The rate constants (k_{obs}) were then determined by plotting the natural logarithm of the fraction of DNA that remains uncleaved versus the reaction time. The negative slope of the line produced by a least-squares fit to the data was taken as the rate constant. 'ET1/S2' represents the *trans* deoxyribozyme at ET1/S2 ratio of 50:1. Two independent experiments were carried out for each deoxyribozyme construct (shown as the second and third columns; the fourth column is the average value. 'S1 only' represents the rate constant of the uncatalyzed reaction ($k_{backgroud}$). The rate enhancement (the last column) was calculated by dividing k_{obs} of a concerned deoxyribozyme with $k_{backgroud}$.

We also measured the rate constant for the spontaneous cleavage of the substrate S1 as an approximation of the uncatalyzed reaction rate under our experimental conditions ($k_{uncatalyzed}$). The plot for the rate determination is shown in Figure 8B. It is worth commenting that we used a highly radioactive, 5′-^{32}P-phosphorylated S1 so that the cleavage product could still be detected by a Phosphorimager after several weeks of decay. The analysis of the cleavage products from two independent reactions incubated for up to 28 days revealed that the spontaneous cleavage rate of S1 was 6.0×10^{-7} min^{-1}. As a comparison, the spontaneous RNA cleavage at pH 7 and 23°C under similar salt concentrations was previously reported to have a rate constant of $\sim 1 \times 10^{-8}$ min^{-1} (29).

The rate enhancements of the deoxyribozymes featured in Table 1 were estimated by $k_{obs}/k_{uncatalyzed}$ and are listed as the last column of the table. The original pH4DZ1 and several members of '+++++' class exhibit a rate enhancement of $\sim 10^6$-fold, equaling the performance by the well-known 10–23 deoxyribozyme that is capable of cleaving RNA in the neutral pH range (8,14). This analysis clearly indicates that the catalytic power of DNA is fully retained even in a highly acidic solution.

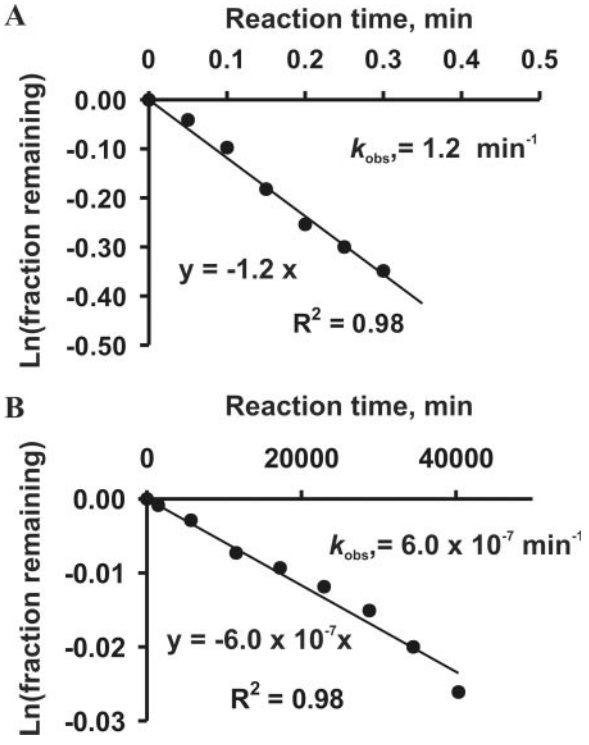

Figure 8. Determining catalyzed and uncatalyzed RNA cleavage reaction rates at pH 3.8. (**A**) Plot for deriving the initial rate constant of EC6 as a representative deoxyribozyme. The *cis* deoxyribozyme was allowed to cleave in the selection/assay buffer. The reaction was stopped at certain time intervals to obtain data points under 20% reaction completion. The natural logarithm of the fraction of DNA that remains cleaved (*y*-axis) is then plotted against the reaction time (*x*-axis). (**B**) Plot for deriving the background rate. The *x*-axis represents reaction time in min and *y*-axis plots natural logarithm of the fraction of S1 that remained uncleaved at the various reaction times. Each data point in both plots represents the average value of two independent experiments. The negative slope of the least-squares fit is taken as the first-order initial rate constant.

DISCUSSION

Undoubtedly, DNA, which is composed of only four chemically analogous building blocks with extremely limited chemical functionalities, is and should be viewed as a polymer that is far less fit for catalysis than protein molecules that are made of 20 functionality-diverse amino acids. However, it has been well demonstrated that catalytic DNAs can be conveniently derived in research laboratories by *in vitro* selection. In fact, human creativity has led to many surprising findings with regard to the catalytic aptitude of DNA. For example, the most well-known RNA-cleaving DNA enzyme 10–23 is not only small in size (which contains a catalytic core built of only 15 nt) but can also perform site-specific RNA cleavage with a k_{cat} of $\sim$10 min^{-1}, k_{cat}/K_M of $\sim 10^9$ M^{-1} min^{-1} and a rate enhancement of $\sim 10^6$ (8,14). Another example is a small DNA-adenylating deoxyribozyme known as the 'class I DNA capase' that exhibits a rate enhancement of 10^{10}-fold (11). Accumulative evidence has convincingly shown that DNA, despite its simplicity in chemical functionality, still possesses considerable capacity for enzymatic function (1–5). Therefore, studying the catalytic ability of DNA can reveal useful information that will enhance our understanding of phenomenon of catalysis itself.

The experiments described in this study were designed to appreciate the catalytic and sequence properties of pH4DZ1, an unusual DNA catalyst that was specifically evolved to perform catalysis at pH $\sim$4—a rather challenging chemical condition. Our results have shown that pH4DZ1 can perform the given task with a surprising proficiency, reflected both by its catalytic rate constant of $\sim$1 min^{-1} and the rate enhancement of $\sim 10^6$-fold. The fact that both parameters are comparable to 10–23—the best deoxyribozyme known to date that operates at neutral pH range—strongly suggests that the catalytic power of DNA is retained at high acidity.

There are some noticeable differences between neutral and acidic deoxyribozymes. First, neutral deoxyribozymes such as 10–23 and 8–17 are extremely small in size. Both 10–23 and 8–17 contain a catalytic core of about a dozen nucleotides and two substrate binding arms of about 6–8 nt. In other words, these two deoxyribozymes are made of less than 30 nt. Our sequence truncation experiments above have shown that pH4DZ1 is a much larger deoxyribozyme that requires $\sim$80 nt for the optimal catalytic activity. Second, all neutral RNA-cleaving deoxyribozymes (including 10–23 and 8–17) explore Watson–Crick base pairing interactions for substrate binding (8,14–16,23–28,30–33). It is expected that the Watson–Crick rules do not apply to DNA at acidic pH range because of extensive protonation at the N1 atom of adenosine and the N3 atom of cytosine (both of which are hydrogen-bonding sites in Watson–Crick base pairs). Indeed, we failed to confirm the possible Watson–Crick helices predicted by *mfold* (data not shown) (34). Therefore, we can conclude that Watson–Crick base pairing rules do not apply to pH4DZ1. The lack of simple yet effective Watson–Crick interactions may explain why pH4DZ1 is much a larger deoxyribozyme than 10–23 or 8–17: the tertiary structure of pH4DZ1 is likely constructed using much more complex interaction network that involves several structural domains and many distal nucleotides. The third difference is that all the neutral *trans*-acting RNA-cleaving deoxyribozymes have excellent multiple-turnover capability while the engineered *trans*-acting pH4DZ1 has somewhat poorer ability in this regard. We have not determined the precise reasons for the smaller multiple-turnover rate observed for pH4DZ1. It is possible that the interactions that govern the substrate-deoxyribozyme recognition for pH4DZ1 are considerably different from the ones exploited by the neutral deoxyribozymes, and as a result, the engineered *trans*-acting system of pH4DZ1 has a slow substrate binding or product release step that is rate limiting. Alternatively, the highly acidic medium and rather high ionic strength may cause severe DNA aggregation, such that only a fraction of the substrate exists in the cleavable form. Detailed kinetic analysis of the *trans*-acting system of pH4DZ1 will be carried out in the future and results will be reported elsewhere.

The original pH4DZ1 contains 123 nt and Figure 9 summarizes the significance of these nucleotides in relation to the catalytic function of the deoxyribozyme, based on the data obtained from both the sequence truncation and reselection experiments. Among the 75 nt required for the optimal function of pH4DZ1 (nucleotides shown in black, blue and red), 53 of them appear to play crucial roles in the function of

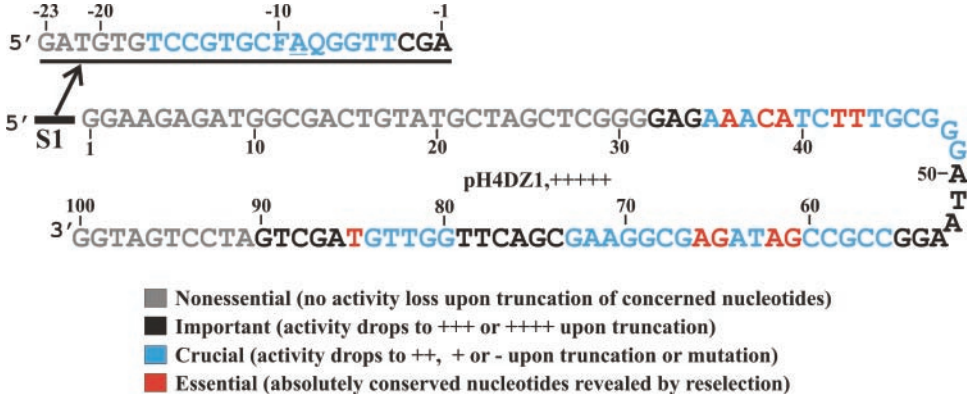

Figure 9. Summary of truncation, mutation and reselection data. The significance of each of the 123 nt within the original pH4DZ1 sequence is categorized using the following coloring scheme: grey: nonessential nucleotides (their truncation causes no activity loss); black: important nucleotides (activity drops by up to 100-fold upon truncation or mutation); blue: crucial nucleotides (activity drops by more than 100-fold upon truncation or mutation); red: essential nucleotides (absolutely conserved nucleotides revealed by the reselection data presented in Figure 4).

the deoxyribozyme (blue and red nucleotides). Ten of these nucleotides are absolutely essential (red nucleotides). Interestingly, these crucial nucleotides are distributed into three sequence elements separated by some important nucleotides (shown in black). The methylation interference experiment shown in Figure 5 supports the notion that these nucleotides are involved in the formation of the active site of the deoxyribozyme: several guanine residues in or near these regions cannot tolerate the methylation at N7 positions while some other guanines are prone to methylation.

The three special nucleotides in the substrate domain—the ribonucleotide, the fluorophore-modified dT (F) and the quencher-modified dT (Q) apparently make important contribution to the structure and/or the function of the deoxyribozyme, reflected by the observations that (i) neither the fluorophore nor the quencher can be removed and (ii) the adenine located on the ribose at the cleavage site cannot be mutated into other bases. We speculate that the active site of the deoxyribozyme is rather complex and involves the ribonucleotide, the fluorophore and the quencher, and some or all of the 10 absolutely conserved nucleotides in the three highly crucial sequence elements. This active site is very likely further supported by the nucleotides that surround the three sequence elements. The precise structure of pH4DZ1 can only be revealed by high-resolution techniques including NMR and X-ray crystallography, which will be the subject of future experimentation.

SUPPLEMENTARY DATA

Supplementary Data are available at NAR Online.

ACKNOWLEDGEMENTS

This work was supported by research grants from the Canadian Institutes for Health Research, MDS-Sciex, the Natural Sciences and Engineering Research Council of Canada, the Canada Foundation for Innovation and the Ontario Innovation Trust for support of this work. Y.L. is a Canada Research Chair. Funding to pay the Open Access publication charges for this article was provided by the Canadian Institute of Health Research.

Conflict of interest statement. None declared.

REFERENCES

1. Joyce,G.F. (2004) Directed evolution of nucleic acid enzymes. *Annu. Rev. Biochem.*, **73**, 791–836.
2. Silverman,S.K. (2004) Deoxyribozymes: DNA catalysts for bioorganic chemistry. *Org. Biomol. Chem.*, **2**, 2701–2706.
3. Achenbach,J.C., Chiuman,W., Cruz,R.P. and Li,Y. (2004) DNAzymes: from creation *in vitro* to application *in vivo*. *Curr. Pharm. Biotechnol.*, **5**, 321–336.
4. Breaker,R.R. (2000) Making catalytic DNAs. *Science*, **290**, 2095–2096.
5. Lu,Y. (2002) New transition-metal-dependent DNAzymes as efficient endonucleases and as selective metal biosensors. *Chemistry*, **8**, 4589–4596.
6. Carmi,N., Balkhi,S.R. and Breaker,R.R. (1998) Cleaving DNA with DNA. *Proc. Natl Acad. Sci. USA*, **95**, 2233–2237.
7. Sreedhara,A., Li,Y. and Breaker,R.R. (2004) Ligating DNA with DNA. *J. Am. Chem. Soc.*, **126**, 3454–3460.
8. Santoro,S.W. and Joyce,G.F. (1997) A general purpose RNA-cleaving DNA enzyme. *Proc. Natl Acad. Sci. USA*, **94**, 4262–4266.
9. Flynn-Charlebois,A., Wang,Y., Prior,T.K., Rashid,I., Hoadley,K.A., Coppins,R.L., Wolf,A.C. and Silverman,S.K. (2003) Deoxyribozymes with 2′-5′ RNA ligase activity. *J. Am. Chem. Soc.*, **125**, 2444–2454.
10. Li,Y. and Breaker,R.R. (1999) Phosphorylating DNA with DNA. *Proc. Natl Acad. Sci. USA*, **96**, 2746–2751.
11. Li,Y., Liu,Y. and Breaker,R.R. (2000) Capping DNA with DNA. *Biochemistry*, **39**, 3106–3114.
12. Li,Y. and Sen,D. (1996) A catalytic DNA for porphyrin metallation. *Nature Struct. Biol.*, **3**, 743–747.
13. Chinnapen,D.J. and Sen,D. (2004) A deoxyribozyme that harnesses light to repair thymine dimers in DNA. *Proc. Natl Acad. Sci. USA*, **101**, 65–69.
14. Santoro,S.W. and Joyce,G.F. (1998) Mechanism and utility of an RNA-cleaving DNA enzyme. *Biochemistry*, **37**, 13330–13342.
15. Li,J., Zheng,W., Kwon,A.H. and Lu,Y. (2000) *In vitro* selection and characterization of a highly efficient Zn(II)-dependent RNA-cleaving deoxyribozyme. *Nucleic Acids Res.*, **28**, 481–488.
16. Peracchi,A. (2000) Preferential activation of the 8-17 deoxyribozyme by Ca(II) ions. Evidence for the identity of 8-17 with the catalytic domain of the Mg5 deoxyribozyme. *J. Biol. Chem.*, **275**, 11693–11697.
17. Liu,Z., Mei,S.H., Brennan,J.D. and Li,Y. (2003) Assemblage of signaling DNA enzymes with intriguing metal-ion specificities and pH dependences. *J. Am. Chem. Soc.*, **125**, 7539–7545.
18. Mei,S.H., Liu,Z., Brennan,J.D. and Li,Y. (2003) An efficient RNA-cleaving DNA enzyme that synchronizes catalysis with fluorescence signaling. *J. Am. Chem. Soc.*, **125**, 412–420.
19. Wang,W., Billen,L.P. and Li,Y. (2002) Sequence diversity, metal specificity, and catalytic proficiency of metal-dependent phosphorylating DNA enzymes. *Chem. Biol.*, **9**, 507–517.
20. Brown,A.K., Li,J., Pavot,C.M. and Lu,Y. (2003) A lead-dependent DNAzyme with a two-step mechanism. *Biochemistry*, **42**, 7152–7161.
21. Jayasena,V.K. and Gold,L. (1997) *In vitro* selection of self-cleaving RNAs with a low pH optimum. *Proc. Natl Acad. Sci. USA*, **94**, 10612–10617.
22. Achenbach,J.C., Jeffries,G.A., McManus,S.A., Billen,L.P. and Li,Y. (2005) Secondary-structure characterization of two proficient kinase deoxyribozymes. *Biochemistry*, **44**, 3765–3774.
23. Shen,Y., Brennan,J.D. and Li,Y. (2005) Characterizing the secondary structure and identifying functionally essential nucleotides of pH6DZ1, a fluorescence-signaling and RNA-cleaving deoxyribozyme. *Biochemistry*, **44**, 12066–12076.
24. Breaker,R.R. and Joyce,G.F. (1994) A DNA enzyme that cleaves RNA. *Chem. Biol.*, **1**, 223–229.
25. Breaker,R.R. and Joyce,G.F. (1995) A DNA enzyme with Mg(II)-dependent RNA phosphoesterase activity. *Chem. Biol.*, **2**, 655–660.
26. Roth,A. and Breaker,R.R. (1998) An amino acid as a cofactor for a catalytic polynucleotide. *Proc. Natl Acad. Sci. USA*, **95**, 6027–6031.
27. Santoro,S.W., Joyce,G.F., Sakthivel,K., Gramatikova,S. and Barbas,C.F., 3rd. (2000) RNA cleavage by a DNA enzyme with extended chemical functionality. *J. Am. Chem. Soc.*, **122**, 2433–2439.
28. Cruz,R.P., Withers,J.B. and Li,Y. (2004) Dinucleotide junction cleavage versatility of 8-17 deoxyribozyme. *Chem. Biol.*, **11**, 57–67.
29. Li,Y. and Breaker,R.R. (1999) Kinetics of RNA degradation by specific base catalysis of transesterification involving the 2′-hydroxyl group. *J. Am. Chem. Soc.*, **121**, 5364–5372.
30. Feldman,A.R. and Sen,D. (2001) A new and efficient DNA enzyme for the sequence-specific cleavage of RNA. *J. Mol. Biol.*, **313**, 283–294.
31. Schlosser,K. and Li,Y. (2004) Tracing sequence diversity change of RNA-cleaving deoxyribozymes under increasing selection pressure during *in vitro* selection. *Biochemistry*, **43**, 9695–9707.
32. Faulhammer,D. and Famulok,M. (1997) Characterization and divalent metal-ion dependence of *in vitro* selected deoxyribozymes which cleave DNA/RNA chimeric oligonucleotides. *J. Mol. Biol.*, **269**, 188–202.
33. Faulhammer,D. and Famulok,M. (1996) The Ca2+ ion as a cofactor for a novel RNA-cleaving deoxyribozyme. *Angew. Chem. Int. Ed. Engl.*, **35**, 2837–2841.
34. Zuker,M. (2003) Mfold web server for nucleic acid folding and hybridization prediction. *Nucleic Acids Res.*, **31**, 3406–3415.